Magnetic hysteresis of Ni nanowires

2000 J. Phys.: Condens. Matter 12 L497

(http://iopscience.iop.org/0953-8984/12/30/103)

J. Phys.: Condens. Matter **12** (2000) L497–L503. Printed in the UK PII: S0953-8984(00)14989-6

LETTER TO THE EDITOR

Magnetic hysteresis of Ni nanowires

M Zheng†, R Skomski†, Y Liu‡ and D J Sellmyer†

† Department of Physics and Astronomy and Center for Materials Research and Analysis, University of Nebraska, Lincoln, NE 68588, USA

‡ Department of Mechanical Engineering and Center for Materials Research and Analysis, University of Nebraska, Lincoln, NE 68588, USA

Received 26 June 2000

Abstract. Magnetization processes in Ni nanowire arrays are investigated. The wires are produced by electrodepositing Ni into porous anodic alumina and exhibit coercivities of the order of 0.05 T (500 Oe) along the wire axis. Transmission-electron microscopy of freed wires shows that the wires are polycrystalline and resemble a chain of nanocrystallites. To model the hysteresis loops, the wires are treated as one-dimensional random-anisotropy magnets where the magnetocrystalline bulk anisotropy is a weak perturbation to the leading anisotropy contribution. The calculation yields an analytical equation for the magnetization as a function of the applied magnetic field. For small and moderate reversed fields, the agreement between theory and experiment is very good, but the applicability of the model breaks down close to the coercive field. This failure is explained by the neglect of higher-order perturbation terms describing, for example, magnetic localization effects.

Periodic arrays of nanoscaled magnetic dots and wires are of great interest as patterned magnetic recording media and sensor devices [1]. They are also ideal systems in which to study magnetic interactions and magnetization processes [2–4]. Current nanofabrication techniques for making such structures include electron-beam [5], interferometric lithography [6] and microprobe-assisted manipulation [7], to expose a controlled electron beam or light to a resist-covered surface or to manipulate atoms by a microprobe. These methods are relatively time consuming and expensive. Another method is electrodeposition of metal into anodic porous alumina, created by anodizing Al in acidic electrolyte, with more or less uniform pore diameters of 10 to 100 nm and spacing of 30 to 120 nm depending on the anodization conditions. Magnetic materials such as Fe, Co and Ni can be electrodeposited into the pores forming magnetic nanowire arrays [3].

A topic of practical and theoretical interest is the modelling of the wires' hysteresis loops [2], which requires knowledge of the wires' real structure and amounts to the calculation of the local magnetization direction as a function of the external magnetic field. From a more general point of view, the theoretical interest in nanowires is linked to the complicated problem of magnetization reversal in real magnets. In fact, nanowires are of particular interest, because their magnetization reversal is not obscured by difficult-to-control bulk domains. Modelling the wires as defect-free long ellipsoids of revolution leads to nucleation fields which are generally larger than the observed coercivities [8, 9]. Since the nucleation modes and fields considered in [8, 9] are exact solutions of the nucleation problem, one has to ascribe the discrepancy between theory and experiment to deviations from the ideal wire shape and structure [10, 11]. The wires considered in this letter are particularly interesting, because their small radius, about 5 nm, corresponds to the coherent-rotation mode rather than to the somewhat more

0953-8984/00/300497+07$30.00

complicated curling mode, and because the wires are well characterized by transmission-electron microscopy (TEM). In this letter, we determine the morphology of Ni nanowire arrays by TEM and compare the observed hysteresis loops with the predictions of a one-dimensional random-anisotropy model.

The preparation of the wire arrays is similar to that described in reference [3]. Briefly, a 99.997% purity Al sheet was used as a starting material; it was first electropolished in a mixed solution of 165 ml 65% $HClO_4$, 700 ml ethanol and 100 ml 2-butoxyethanol and 137 ml H_2O, and then anodized in 15% H_2SO_4 at 10 V dc for 30 min. The Ni nanowires were electrodeposited into the anodized template using an electrolyte containing 0.1 M $NiSO_4 \cdot 6H_2O$ and 45 g l^{-1} boric acid. The electrodeposition of the Ni wires was carried out with an alternating current of 15 V, frequency of 250 Hz and temperature of 55 °C.

Well-ordered nanoarrays are formed by three-step anodization:

(i) anodizing Al at 40 V dc in 3% oxalic acid for about ten minutes and then removing the oxide layer formed by immersion into the mixed chromic and phosphoric acid for 15 minutes,
(ii) anodizing for 12 hours and removing the top oxide layer again, followed by
(iii) a third three-minute anodization step.

Figure 1 shows the atomic force microscopy (AFM) top view of the template after the three-step anodization. When anodizing Al in 15% sulphuric acid, the diameter and spacing are about 10 nm and 35 nm, respectively.

To determine the structure, diameter and length of the Ni nanowires by TEM, the nanowires were released by immersing the specimen in a mixed solution of 0.2 M chromic acid and 0.4 M

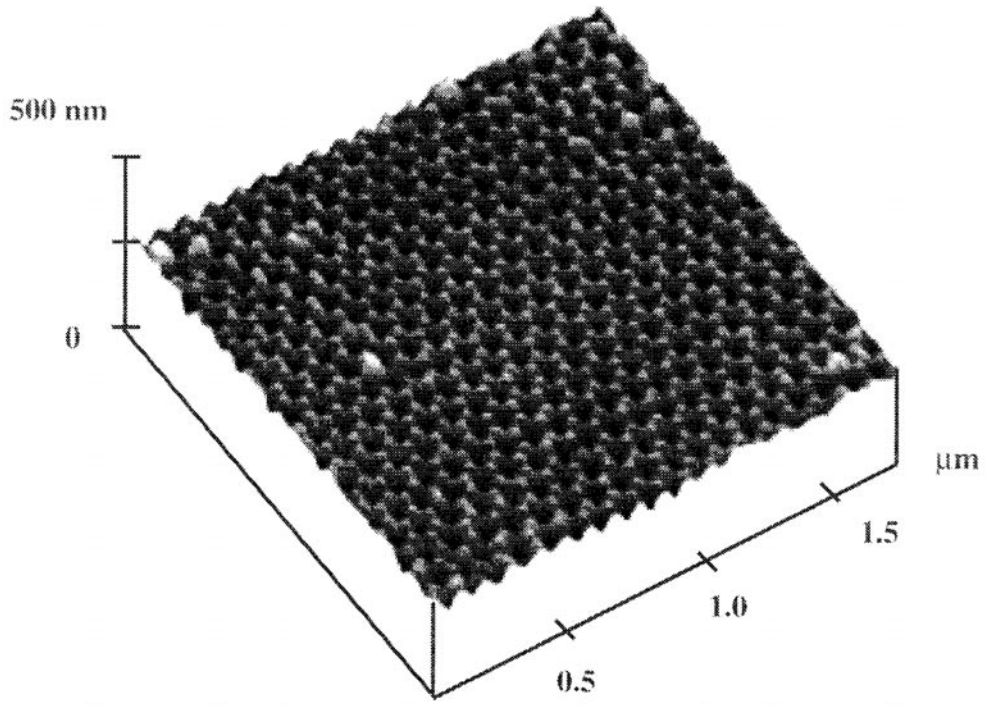

Figure 1. An AFM top view of a nanopore array in anodic alumina prepared by three-step anodization. The anodization was conducted in 3% oxalic acid at 40 V.

phosphoric acid. Figure 2 shows a high-resolution TEM image of single Ni nanowires liberated from the template. Each wire is polycrystalline, consisting of a chain of single-crystalline segments, and the crystallite size is around 10 nm. We also see that the wires' surfaces are not free of defects and inhomogeneities [12]. As emphasized in reference [10], these imperfections are of great importance for the theoretical understanding of nanomagnets.

To investigate the hysteresis behaviour of the wires, magnetic measurements were carried out with an alternating-gradient force magnetometer (AGFM). Magnetic nanowire arrays in alumites exhibit easy magnetization along the wire axis, that is, perpendicular to the film plane, and the coercivity can be as high as 0.048 T (480 Oe) for nanowire arrays with diameter of about 10 nm. The coercivity is ascribed to the comparatively strong shape anisotropy of the wires [2, 13]. To account for the interwire magnetostatic interactions, the external field has been corrected by a demagnetizing field $(-DM)$, where $D \approx f$ is the area (or volume) fraction of the wires in the film [3].

The polycrystallinity of the wires and the rough wire surface (see figure 2) mean that the wires must be treated as random-anisotropy ferromagnets. Random-field [14] and random-anisotropy phenomena have attracted much attention in the past due to their interesting dimensional dependence [15–18]. Essentially, the random preferential magnetization directions of the crystallites (size L) favour magnetization misalignment but must compete against the exchange and external fields, which favour magnetization alignment. Three-dimensional nanostructures have been treated by Chudnovsky *et al* [17], although no hysteresis loops have been calculated. Here we consider the wire as a thin chain of polycrystallites whose grain boundaries are at random positions, the average segment length (grain length) being L. The behaviour of the wires is determined by the competition between interatomic exchange (exchange stiffness A), magnetostatic interactions and magnetic anisotropy (K_{eff}), and we trace the magnetization $\boldsymbol{M}(\boldsymbol{r}) = M_s\boldsymbol{s}(\boldsymbol{r})$ as a function of the external field $\boldsymbol{H} = H\boldsymbol{e}_z$. The starting point is the micromagnetic energy [13]

$$E = \int (A(\nabla \boldsymbol{s})^2 - K_{eff}(\boldsymbol{n}\cdot\boldsymbol{s})^2 - \mu_0 M_s \boldsymbol{H}\cdot\boldsymbol{s})\,\mathrm{d}V \tag{1}$$

where the unit vector $\boldsymbol{n} = \boldsymbol{n}(\boldsymbol{r})$ denotes the (random) local easy axis. The effective anisotropy constant K_{eff} incorporates shape, magnetocrystalline and magneto-elastic anisotropy contributions. Higher-order anisotropy constants are neglected in equation (1), because they are fairly small and do not yield new physics beyond the randomness and non-linearity implied by K_{eff}. Since the wire surface (figure 2(b)) exhibits some randomness, the associated magnetic surface charges add to the random magnetocrystalline anisotropy. Note that due to the assumption of very thin wires, there is no non-local magnetostatic term in equation (1).

The easy axis $\boldsymbol{n}$ closest to $\boldsymbol{e}_z$ and the normalized magnetization vector can be written as

$$\boldsymbol{n}(\boldsymbol{r}) = \sqrt{1 - a^2(\boldsymbol{r})}\boldsymbol{e}_z + \boldsymbol{a}(\boldsymbol{r}) \tag{2}$$

and

$$\boldsymbol{s}(\boldsymbol{r}) = \sqrt{1 - m^2(\boldsymbol{r})}\boldsymbol{e}_z + \boldsymbol{m}(\boldsymbol{r}). \tag{3}$$

Here $\boldsymbol{a}(\boldsymbol{r})$ and $\boldsymbol{m}(\boldsymbol{r})$ are the easy-axis and magnetization components perpendicular to the wire (in the film plane). For not-too-large reverse fields we can restrict our consideration to terms linear in the small quantity $\boldsymbol{m}$. In particular, ignoring a physically irrelevant zero-point energy, we obtain from equation (1) the anisotropy term $-K_{eff}(\boldsymbol{n}\cdot\boldsymbol{s})^2 = -2K_{eff}\boldsymbol{m}\cdot\boldsymbol{a}$. Minimizing the total magnetic energy with respect to $\boldsymbol{m}$ then yields, in one dimension, the linearized differential equation

$$-A\frac{\mathrm{d}^2\boldsymbol{m}}{\mathrm{d}z^2} + \left(K_{eff} + \frac{1}{2}\mu_0 M_s H\right)\boldsymbol{m} = K_{eff}\boldsymbol{a}(z). \tag{4a}$$

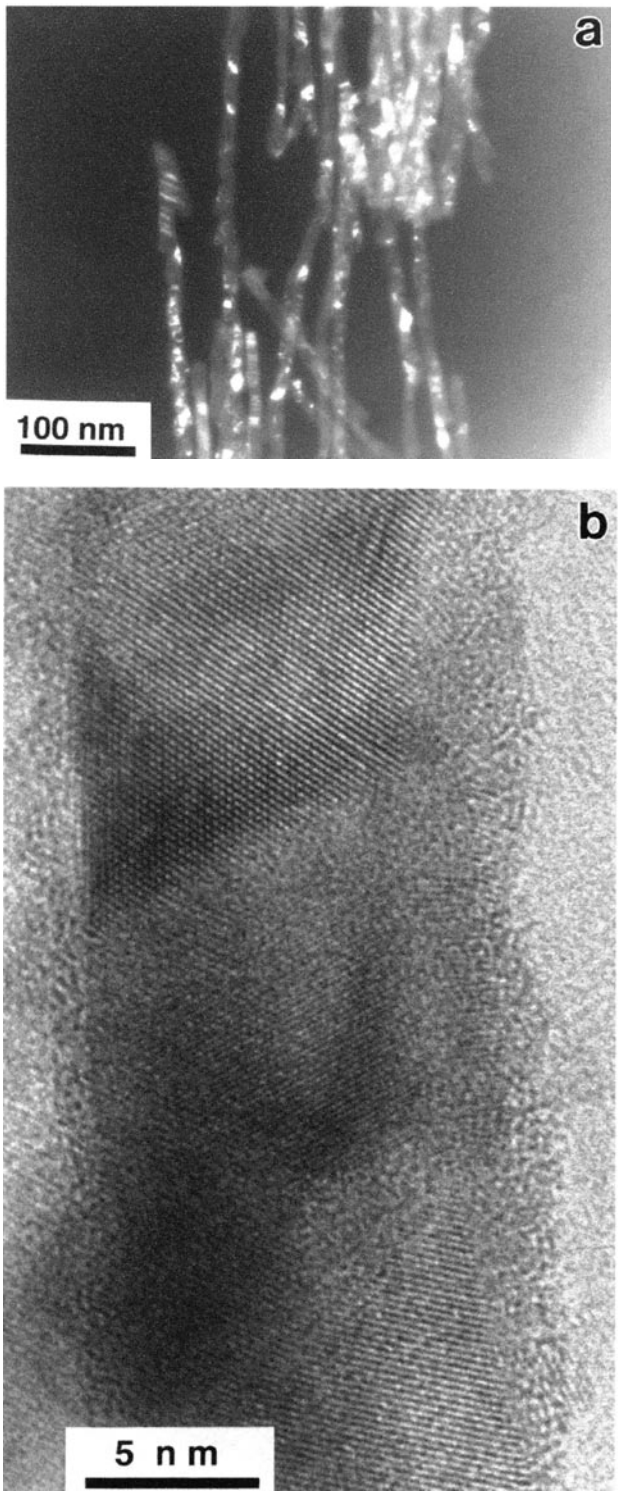

Figure 2. High-resolution TEM micrographs of Ni nanowires liberated from the anodic alumites.

This equation means that the polycrystalline easy-axis disorder $\boldsymbol{a}(z)$ acts as a random inhomogeneity. It can also be written as

$$-\frac{\mathrm{d}^2\boldsymbol{m}}{\mathrm{d}z^2}+\kappa^2\boldsymbol{m}=\boldsymbol{f}(z) \tag{4b}$$

where

$$\kappa^2=\frac{K_{eff}}{4A}\left(1+\frac{H}{H_0}\right) \tag{5}$$

and $\boldsymbol{f}(z)=K_{eff}\boldsymbol{a}(z)/A$. Note that the parameter $H_0=2K_{eff}/\mu_0 M_s$ is the anisotropy field corresponding to K_{eff}.

The formal solution of equation (4*b*) is

$$\boldsymbol{m}(z)=\frac{1}{2\kappa}\int_{-\infty}^{+\infty}\exp(-\kappa|z-\xi|)\boldsymbol{f}(\xi)\,\mathrm{d}\xi. \tag{6}$$

Due to equation (3), the magnetization, averaged over the wire length, is given by

$$M(H)=\langle M_z\rangle=M_s\left(1-\frac{\langle\boldsymbol{m}^2(z)\rangle}{2}\right) \tag{7}$$

where higher-order terms associated with equations (1) and (3) are neglected.

The main problem is now that of evaluating the average $\langle\boldsymbol{m}^2(z)\rangle$. Since we assume that the grain boundaries are randomly distributed, the correlation function is given by $\langle\boldsymbol{a}(0)\cdot\boldsymbol{a}(z_0)\rangle=c_0\exp(-z_0/L)$.

In this equation, the parameter $c_0=\langle\boldsymbol{a}^2\rangle$ describes the strength of the wire disorder and incorporates both magnetocrystalline and magnetostatic contributions. For the case considered of nearly ideal wires we expect c_0 to be much smaller than 1. The average magnetization is given by

$$\langle\boldsymbol{m}^2(z)\rangle=\frac{c_0K_{eff}^2}{4A^2\kappa^2}\int_{-\infty}^{+\infty}\int_{-\infty}^{+\infty}\exp(-\kappa|z-\xi|-\kappa|z-\eta|-|\xi-\eta|/L)\,\mathrm{d}\eta\,\mathrm{d}\xi. \tag{8}$$

The double integral in equation (8) has the value $2(2\kappa+1/L)/[\kappa(\kappa+1/L)^2]$, so, with equation (7),

$$M(H)=M_s\left(1-\frac{c_0K_{eff}^2(2\kappa+1/L)}{4A^2\kappa^3(\kappa+1/L)^2}\right). \tag{9}$$

In this equation, the field dependence is hidden in $\kappa(H)$. This equation can be rewritten as

$$M(H)=M_s\left(1-\frac{c_0K_{eff}^2}{4A^2}\left\{\left[2\sqrt{\frac{K_{eff}}{A}}\sqrt{1+\frac{\mu_0M_sH}{2K_{eff}}}+\frac{1}{L}\right]\right.\right.$$
$$\left.\left.\times\left[\left(\frac{K_{eff}}{A}\right)^{3/2}\left(1+\frac{\mu_0M_sH}{2K_{eff}}\right)^{3/2}\left(\sqrt{\frac{K_{eff}}{A}}\sqrt{1+\frac{\mu_0M_sH}{2K_{eff}}}+\frac{1}{L}\right)^2\right]^{-1}\right\}\right) \tag{10}$$

where $\kappa=\kappa_0\sqrt{1+\mu_0M_sH/2K_{eff}}$ and $\kappa_0=\sqrt{K_{eff}/A}$.

Figure 3 compares the prediction of equation (10) with the experimental hysteresis loops of nanowires having radii of about 5 nm. The best fit is obtained for $c_0=0.16$ and $K_{eff}=0.035$ MJ m^{-3}. From figure 3 we see that the agreement between theory and experiment is excellent unless we approach H_c. In particular, equation (10) exhibits singularity for $H<H_0$ and leads to the unphysical prediction that $M(-H_0)=-\infty$. The physics behind this singularity is the instability of the original magnetization state at the nucleation field. The incorrect description of the coercivity is due to the neglect of higher-order perturbation corrections in equation (4):

(i) the linear character of equation (4) limits the applicability of the theory to small $\boldsymbol{m}$ and $M_s - \langle \boldsymbol{m}_z \rangle \ll M_s$ and
(ii) equation (4) ignores the micromagnetic localization of the reversal process.

The localization originates from the neglect of higher-order $\boldsymbol{a}$-dependent corrections to κ: since $\boldsymbol{a}$ depends on $\boldsymbol{r}$, these corrections modify the partial differential equation (4*b*) and its eigenmode behaviour. A consequence is the localization of the eigenmode responsible for nucleation [11, 13] and the coercivity reduction shown in figure 3†.

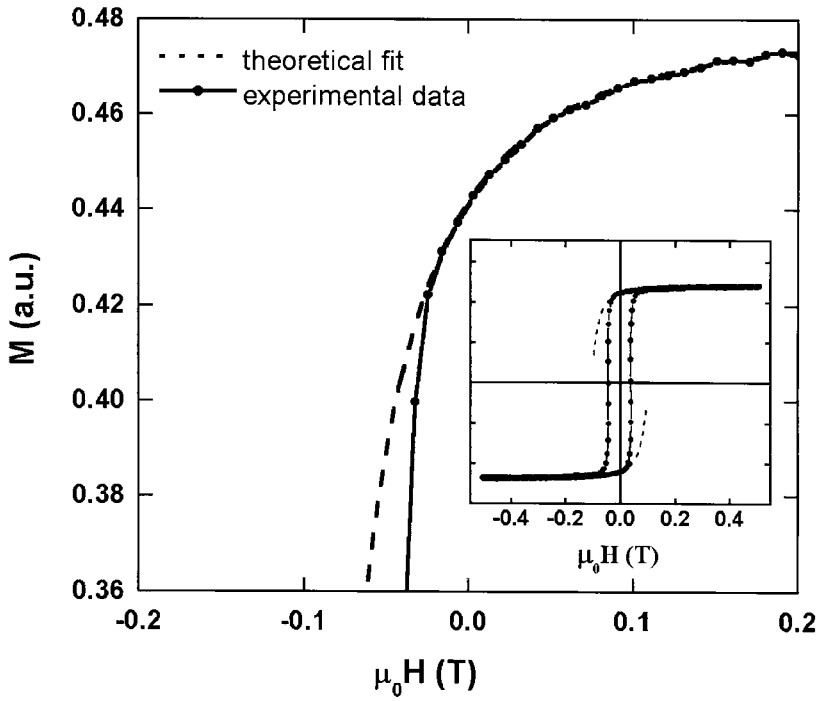

Figure 3. A theoretical fit for the hysteresis loop of Ni nanowire arrays. The inset shows that the theory overestimates the coercivity.

The fitted parameter $K_{eff} = 0.035$ MJ m^{-3} is similar to the maximum shape anisotropy constant $\mu_0 M_s^2/4 = 0.078$ MJ m^{-3}. Writing $K_{sh} = (1-3D)\mu_0 M_s^2/4$, we see that $K_{eff} = K_{sh}$ for $D \approx 0.14$. This indicates that finite-thickness effects are not properly described in the present theory: for infinitely thin wires we would obtain $D = 0$. For the same reason, the present approach cannot be used to discuss the comparatively weak thickness dependence of the coercivity. The value $c_0 = 0.16$ indicates random magnetostatic forces at the wire surface due to disorder. For pure magnetocrystalline disorder, c_0 would be of the order of 0.02, but magnetostatic charges at the wires' rough surface (figure 2) give rise to random-anisotropy contributions dominating the comparatively weak Ni bulk anisotropy ($K_1 = -0.005$ MJ m^{-3}).

In conclusion, we have investigated the magnetization processes in thin Ni nanowires fabricated by electrodeposition. The wires have radii as small as 5 nm, so interatomic exchange ensures a largely coherent magnetization state perpendicular to the wire axis. Transmission-

† An analysis of micromagnetic localization in nanowires will be published elsewhere. Note that the 'failure' of the present theory is relative: the overestimation of H_c by a factor of order 2 must be compared with the overestimation by a factor of 10 or more for other materials (see e.g. reference [13]).

electron micrography performed on freed wires shows that the wires are polycrystalline with crystallite sizes of the order of 10 nm. To model the hysteresis loop, the wires are considered as one-dimensional random-anisotropy magnets, that is, as chains of nanocrystallites. Treating the magnetocrystalline bulk anisotropy and the surface disorder as a weak perturbation to the leading shape anisotropy yields an analytical equation for the magnetization as a function of the applied magnetic field. For small and moderate reverse field, the theoretical hysteresis loop predictions agree well with experiment, but the coercivity is significantly larger than predicted. The disagreement is explained by non-linear and localization effects which are contained in equation (1) but ignored in the linear approximation equations (2) to (10). In particular, polycrystalline and surface-related wire imperfections modify the eigenvalue spectrum of the micromagnetic equation and are very effective in reducing the coercivity.

The authors would like to thank Dr L Menon and H Zeng for their help with sample preparation. This work was supported by NSF and CMRA.

References

[1] Chou S Y, Krauss P R and Renstrom P J 1996 *Science* **272** 85
[2] Ferré R, Ounadjela K, George J M, Piraux L and Dubois S 1997 *Phys. Rev.* B **56** 14 066
[3] Zeng H, Zheng M, Skomski R, Sellmyer D J, Liu Y, Menon L and Bandyopadhyay S 2000 *J. Appl. Phys.* at press
[4] Wernsdorfer W, Doudin B, Mailly D, Hasselbach K, Benoit A, Meier J, Ansermet J-Ph and Barbara B 1996 *Phys. Rev. Lett.* **77** 1873
[5] Smith J F, Schultz S, Fredkin D R, Kern D P, Pishton S A, Schmid H, Cali M and Koehler T R 1991 *J. Appl. Phys.* **69** 5262
[6] Kirsch S, Pollmann A, Thielen M, Weinforth H, Carl A and Wassermann E F 1997 *J. Appl. Phys.* **81** 5474
[7] Wirth S, von Molnár S, Field M and Awschalom D D 1999 *J. Appl. Phys.* **85** 5259
[8] Aharoni A 1996 *Introduction to the Theory of Ferromagnetism* (Oxford: Oxford University Press)
[9] Aharoni A 1997 *J. Phys.: Condens. Matter* **9** 10 009
[10] Aharoni A 1999 *J. Magn. Magn. Mater.* **203** 33
[11] Skomski R 1998 *J. Appl. Phys.* **83** 6724
[12] There are, for example, difficult-to-quantify surface-anisotropy contributions associated with the lattice planes shown in figure 2(b); see e.g.
Millev Y, Skomski R and Kirschner J 1998 *Phys. Rev.* B **58** 6305
[13] Skomski R and Coey J M D 1999 *Permanent Magnetism* (Bristol: Institute of Physics Publishing)
[14] Imry Y and Ma Sh-K 1975 *Phys. Rev. Lett.* **35** 1399
[15] Sellmyer D J and Nafis S 1986 *Phys. Rev. Lett.* **57** 1173
[16] Alben R, Becker J J and Chi M C 1978 *J. Appl. Phys.* **49** 1653
[17] Chudnovsky E M, Saslow W M and Serota R A 1986 *Phys. Rev.* B **33** 251
[18] Skomski R 1996 *J. Magn. Magn. Mater.* **157+158** 173